DRL NO. 77 - DOE/JPL - 955307
Distribution Category UC-63

ANALYSIS OF THE EFFECTS OF IMPURITIES IN SILICON

FINAL REPORT

FOR PERIOD COVERING

19 JANUARY 1979 TO 31 JANUARY 1980

BY

J. H. WOHLGEMUTH
M. N. GIULIANO

JPL CONTRACT NO. 955307

SOLAREX CORPORATION
1335 PICCARD DRIVE
ROCKVILLE, MD 20850

SOLAREX CORPORATION

DRL NO. 77 - DOE/JPL - 955307
Distribution Category UC-63

ANALYSIS OF THE EFFECTS OF IMPURITIES IN SILICON

FINAL REPORT

FOR PERIOD COVERING

19 JANUARY 1979 TO 31 JANUARY 1980

BY

J. H. WOHLGEMUTH
M. N. GIULIANO

JPL CONTRACT NO. 955307

SOLAREX CORPORATION
1335 PICCARD DRIVE
ROCKVILLE, MD 20850

"The JPL Low-Cost Solar Array Project is sponsored by the U.S. Department of Energy and forms part of the Solar Photovoltaic Conversion Program to initiate a major effort toward the development of low-cost solar arrays. This work was performed for the Jet Propulsion Laboratory, California Institute of Technology by agreement between NASA and DOE."

ABSTRACT

The purpose of this program was to conduct a solar cell fabrication and analysis program to determine the effects on the resultant solar cell efficiency of impurities intentionally incorporated into silicon. The program employed "flight-quality" technologies and quality assurance typical of an experienced solar cell manufacturer to assure that variations in cell performance are due to the impurities incorporated in the silicon. A rigid program of documentation and decontamination procedures was instituted. Four different types of cell lots were processed:

- Verification lots which established a baseline process
- Monitor cells which preceded the test runs and established a clean processing system
- Control cells which were processed simultaneous with the test cells
- Test cells as supplied by JPL and which contained contaminants the nature of which was not revealed to Solarex until after processing and measurement of each subgroup.

The cells from control silicon including verification, monitor and control cells have exhibited average AM0 cell efficiencies of nearly 13% at 25°C (in excess of 15% AM1 at 25°C). No cross-contamination of control or monitor cells was observed.

Cells with various doping materials and doping levels were fabricated. The test cells appear to be clustered in two distinct resistivity ranges, namely around 0.2 Ω-cm and between 3.0 and 5.0 Ω-cm. The lower-resistivity cells in general exhibit higher open-circuit voltages and lower short-circuit currents than the control cells (1.0 to 3.0 Ω-cm). The higher-resistivity cells exhibit lower open-circuit voltages. The short-circuit current is much more susceptible to change by impurity incorporation than the open-circuit voltage although several lots have shown severe degradation of both current and voltage. Further study with control wafers in the same resistivity range would be required to clear up any ambiguity due to differences in starting resistivity. There was ample evidence, however, that certain impurities such as titanium, tantalum, and vanadium are particularly bad even in very small concentrations. Cell performance appears relatively tolerable to impurities such as copper, carbon, calcium, chromium, iron and nickel in the concentration levels which we considered.

TABLE OF CONTENTS

1.0 INTRODUCTION AND SUMMARY

One of the major costs of a silicon solar cell is the cost of the high purity silicon that is used as the substrate. There has been a great deal of work done in attempting to define the silicon purity level actually required to produce high efficiency solar cells. Silicon crystals with intentionally added impurities have been grown by both Westinghouse/Dow-Corning[1] and Monsanto[2]. This material has been evaluated by these organizations for impurity content and minority carrier lifetime. While solar cells have been processed under the Westinghouse/Dow-Corning program, the material was not subjected to a standard solar cell manufacturing process. The work reported herein utilizes such a standardized process, which has been used to produce many thousands of terrestrial solar cells, modified to include a higher level of quality control. Silicon wafers which had been grown under the Westinghouse/Dow-Corning program were supplied to Solarex by JPL.

The purpose of this program was to conduct a solar cell fabrication and analysis program to determine the effects on the resultant solar cell efficiency of the impurities intentionally incorporated into the silicon. A "flight-quality"

solar cell process was employed with a stringent quality assurance program. The Solarex program was formulated under the following requirements:

1) Assurance must be given that lots did not get misplaced. Only one lot was ever in process at any given time. Control and test wafers were distinguished by size and identification numbering.

2) The processes must be well controlled and documented to assure that the results are not process dependent. A cell process sequence was selected that has been employed in large scale production. Important process parameters were identified and an in-line Q.A. procedure developed as part of the over-all Q.A. Plan.

3) Decontamination procedures must be incorporated to assure that the lots do not cross-contaminate each other. A cleaning procedure was established. A monitor run was performed before each test run to assure the cleanliness of the process equipment.

4) Finished cells must be subjected to sufficient measurement techniques that the mechanism of impurity effects on cell behavior can be identified.

A number of measurement techniques were chosen for use and decisions made on which techniques were performed on all cells and which were performed on selected samples. A data base for all measurements was established using control wafers during initial verification runs. Then test measurements were compared to this data base.

During the first quarter the Program Plan including the detailed Quality Assurance Plan was developed and submitted to JPL. Various equipment and tooling required for handling and decontaminating the cell processing equipment was identified, ordered and installed. The personnel responsible for cell fabrication were educated in the process sequence procedures, controls and required measurements and the initial verification runs using control or standard silicon were begun.

During the second quarter the program included 1) completion of the processing of verification cells, 2) study of the dependence of cell performance on crystal orientation, and 3) completion of the first five test lots. The various evaluation parameters employed in the program were defined and measurement techniques were described. Included also during this period was a description of the analysis and statistical methods which were employed.

During the third quarter and beyond, processing and analysis were continued on test lots through E-31 and also Lot E-39 which served as baseline material supplied by JPL.

One of the most important aspects of the program was the assurance that the results were dependent on the test material rather than on variations in processing. For this reason, monitor and control cells were fabricated and their performance was continually checked against the verification cell results. In addition, a number of evaluation measurements were performed on selected test and control cells. These results are especially important in evaluating the quality of the anti-reflective coating and of the metallization. The direct measurements of reflection and series resistance have conformed the consistency of the processing and the validity of the experiments to date.

The cells from control silicon including verification, monitor and control cells have exhibited average AMO cell efficiencies of nearly 13% at 25°C (in excess of 15% AM1 at 25°C). No cross-contamination of control or monitor cells has been observed.

Cells with various doping materials and doping levels have been fabricated. The test cells appear to be clustered in two distinct resistivity ranges, namely around 0.2 Ω-cm and between 3.0 and 5.0 Ω-cm. The lower-resistivity cells in

general exhibit higher open-circuit voltages and lower short-circuit currents than the control cells (1.0 to 3.0 Ω-cm). The higher-resistivity cells exhibit lower open-circuit voltages. The short-circuit current is much more susceptible to change by impurity incorporation than the voltage although several lots have shown severe degradation of both current and voltage. Data is tabulated in the report as to degradation resulting from the various impurities both singly and in instances of multiple contamination. For many of the impurity additions, degradation was as severe as 50 percent or more loss in maximum output power for the test cells, with varying degrees of shunting and excess junction current. A number of added impurity samples indicated relatively small degradation effects. The results from Lot E-39, which was uncontaminated material supplied by JPL as baseline material, indicated excellent control of the experiment. This lot was run at the very end of the program and the results were practically indistinguishable from the control wafers. Test wafer data for this lot is included in the Appendix. Also included in the Appendix are test wafer data for Lots E-20 through E-31; data from these lots were accumulated since submission of the last quarterly report.

2.0 Technical Discussion

2.1 Program Description

During the course of the program four different types of cell lots were processed. These cells are identified as:

- Verification Cells - These cells were processed during the first few weeks of the program using control silicon. These runs were designed to verify that cell processes were being performed correctly, to establish control procedures and the Q.A. plan and finally to establish a baseline for all solar cell parameters. The verification runs employed 3-inch diameter wafers that were cut into 2 cm x 2 cm cells. To serve as a data base a minimum number of in-specification verfication runs were required. The minimum number was set at 6. This, however, does not mean that only 6 verification runs were performed, since there were minor variations in parameters and specifications during the early runs. Therefore, sufficient verification runs were processed until 6 successful runs were completed using identical process parameters. The performance characteristics of the verification lots are summarized in the section on cell fabrication (§ 2.1.2).

- Test Cells - These are cells fabricated from the test wafers supplied by JPL containing known quantities of impurities. (At the time of processing Solarex personnel did not know the impurity content of the wafers.) The test wafers were also cut into 2 cm x 2 cm cells.

- Control Cells - These cells were co-processed with the test cells on control silicon. They were used to assure that the processing of each test lot was correct. The control runs employed 3-inch diameter wafers, that were cut into 2 cm x 2 cm cells.

- Monitor Cells - These cells were processed using control silicon after the decontamination procedure was completed. Before each test lot was run, a monitor lot was run and the results analyzed to assure that the equipment was not contaminated. The monitor runs employed 3-inch diameter wafers, that were cut into 2 cm x 2 cm cells.

  If at anytime the results of a monitor lot indicated continued contamination, the decontamination procedure was repeated and then another monitor lot processed. An experimental lot was never run until after the successful completion of a monitor lot.

2.1.1 Process Sequence

The processing of the cells for this program must be performed by a process sequence that is:

- reproducible with minimum batch-to-batch variation
- tolerant of small (unavoidable and/or statistical) variations
- indicative of results expected from "typical" terrestrial cell production.

Under these constraints, Solarex chose a process sequence as shown in the flow chart in Figure 1. This is a process sequence that has been employed for the fabrication of a large number of cells including the fabrication of thin cells for the NASA OAST pilot line, with stringent controls over the process parameters.

2.1.2 Verification Cells

Summary of the AMO I-V measurements on the final 6 verification lots are included in Table 1. The average efficiency of the verification lots is 12.9% (AMO at 25^{o}C). Process evaluation parameters are summarized in Table 2 for the 6 verification lots. This data indicates that the cell processing is consistent from lot to lot. This data base was used as a baseline for the experimental runs.

FIGURE 1

PROCESS SEQUENCE

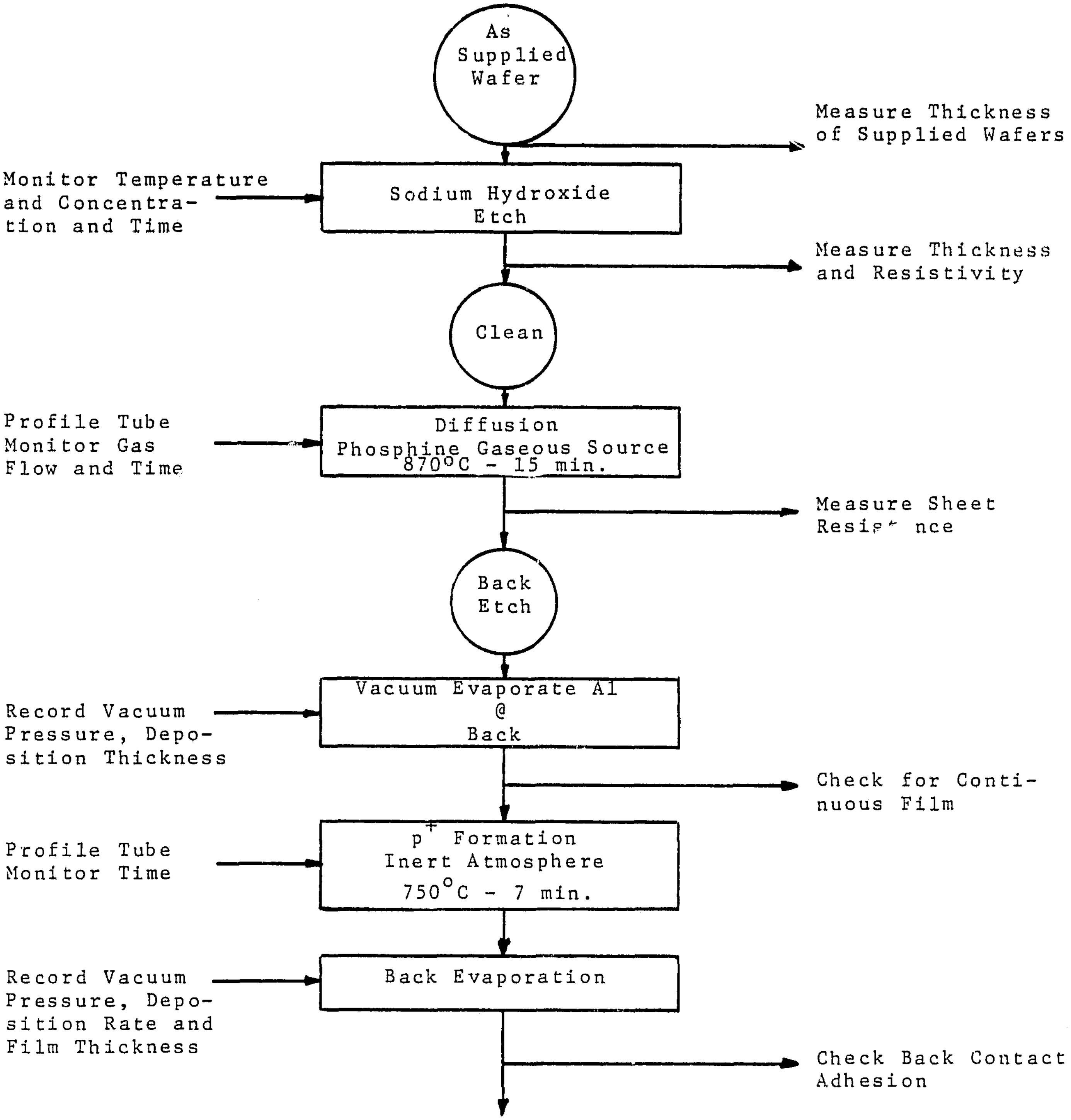

continued on next page

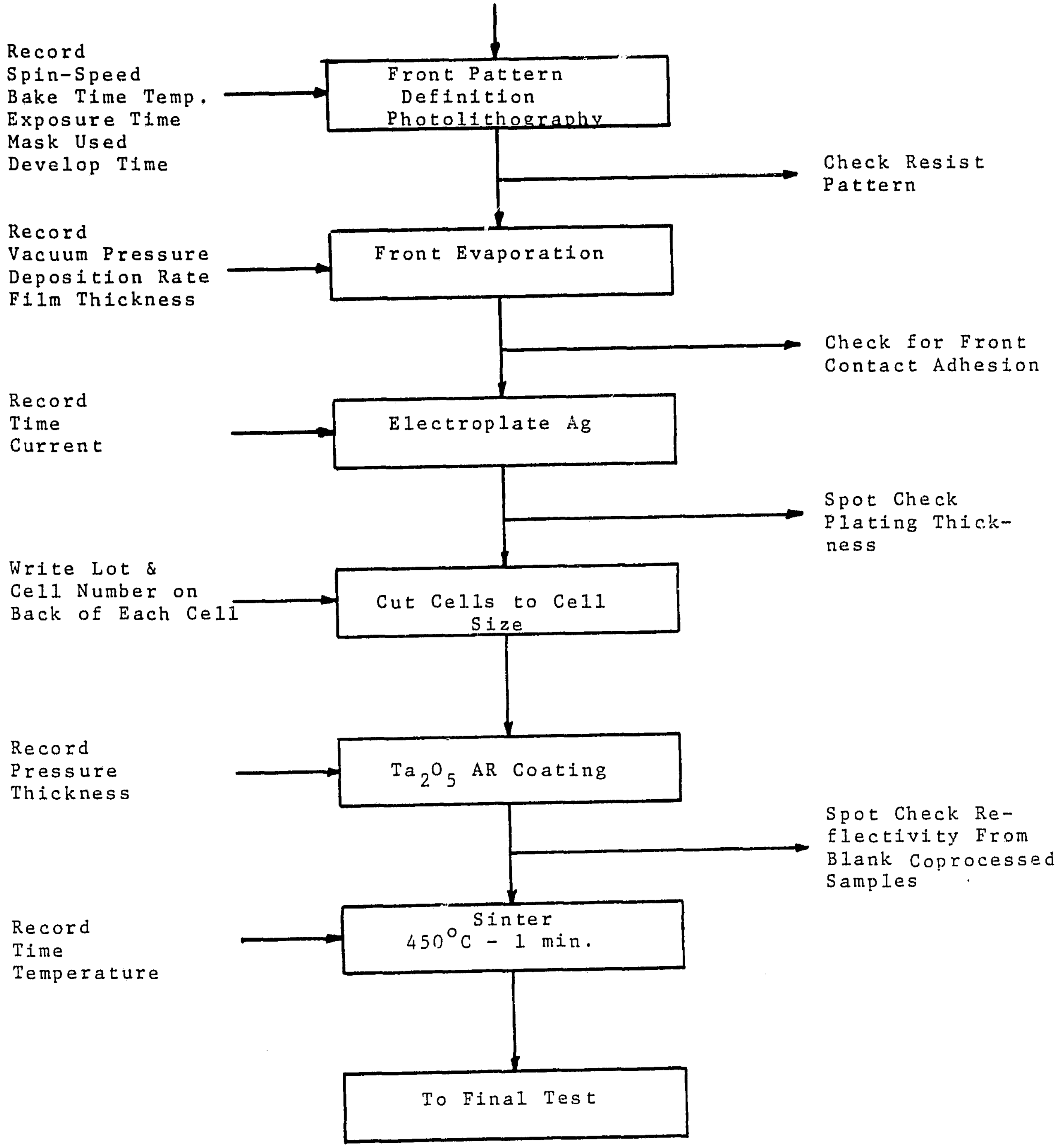
Record
Spin-Speed
Bake Time Temp.
Exposure Time
Mask Used
Develop Time
Front Pattern Definition Photolithography
Check Resist Pattern
Record
Vacuum Pressure
Deposition Rate
Film Thickness
Front Evaporation
Check for Front Contact Adhesion
Record
Time
Current
Electroplate Ag
Spot Check Plating Thickness
Write Lot & Cell Number on Back of Each Cell
Cut Cells to Cell Size
Record
Pressure
Thickness
Ta_2O_5 AR Coating
Spot Check Reflectivity From Blank Coprocessed Samples
Record
Time
Temperature
Sinter
$450^{\circ}C$ - 1 min.
To Final Test

TABLE I

SUMMARY OF VERIFICATION LOTS V-4,-5,-6,-7,-8,-10

Red = Corning #2408
Blue = Corning #9788

Lot #	Isc mA	Voc mV	Pmax. mW	Imp mA	Vmp mV	Isc Blue mA	Isc Red mA	Fill Factor %
V-4 (33 cells)								
AVG.	148.9	595.7	69.0	139.1	496.0	39.9	82.5	77.8
σ	1.72	1.95	2.00	3.44	7.43	1.57	1.30	--
Coef. Var.	.012	.003	.029	.025	.015	.039	.016	--
V-5 (36 cells)								
AVG.	149.1	595.6	68.9	138.8	496.1	39.2	83.3	77.6
σ	1.46	1.15	2.38	4.58	10.85	1.12	.94	--
Coef. Var.	.010	.002	.035	.033	.022	.029	.011	--
V-6 (34 cells)								
AVG.	152.4	597.7	71.1	143.1	497.6	40.7	83.2	78.2
σ	1.10	1.53	1.34	2.41	5.10	1.34	.99	--
Coef. Var.	.007	.003	.019	.017	.010	.033	.012	--
V-7 (27 cells)								
AVG.	149.3	595.7	69.6	140.0	496.9	37.6	84.7	78.2
σ	1.70	2.06	1.33	2.67	4.83	1.39	1.06	--
Coef. Var.	.011	.003	.019	.019	.010	.037	.013	--
V-8 (38 cells)								
AVG.	151.4	594.0	69.9	141.6	506.3	37.4	85.5	79.7
σ	1.88	2.17	2.21	3.92	11.27	2.62	1.70	--
Coef. Var.	.012	.004	.032	.028	.022	.070	.020	--
V-10 (37 cells)								
AVG.	151.3	591.5	70.2	141.2	496.3	38.2	85.0	78.3
σ	1.63	1.97	1.29	1.98	4.15	1.05	1.80	--
Coef. Var.	.011	.003	.018	.014	.008	.027	.021	--
Σ6 Lots								
AVG.	150.4	595.0	69.8	140.6	498.2	38.8	84.0	78.3
σ	1.48	2.09	.818	1.64	4.01	1.32	1.19	.74
Coef. Var.	.010	.004	.012	.012	.008	.034	.014	.009

TABLE 2

PROCESS EVALUATION MEASUREMENT FOR THE VERIFICATION LOTS

Lot No.	Pmax mA	Photon Abs.Effic. α in %	Quantum Yield λ max μ	Quantum Yield % Q Y atλmax	Carriers Collected Per Absb. Photon	Junction Cap. MF	Junction Cond. M℧	R_{series} Ω	R_{shunt} KΩ	Diode Factor n	Io mA
V-4	69.0	.91	.6	89	.82	.115	.03	.074	50.8	1.02	$3X1^{-8}$
V-5	68.9	.91	.6	93	.84	.11[illegible]	2.96	.046	0.345	1.05	$3X10^{-8}$
V-6	71.1	.91	.6	91	.83	.116	.24	.063	4.71	1.05	$3X10^{-8}$
V-7	69.6	.91	.6	92	.84	.093	.29	.089	11.6	1.02	$3X10^{-8}$
V-8	69.9	.91	.65	93	.85	.117	.47	.099	1.56	1.10	$5X10^{-8}$
V-10	70.2	.92	.65	90	.81	.111	.35	.092	4.96	1.10	$5X10^{-8}$

2.1.3 Crystal Orientation Dependence

The initial process sequence was developed using a NaOH etch designed for 100 silicon. Upon completion of the verification runsit was discovered that the test wafers were all from ingots grown from 111 seeds. Therefore the etch procedure had to be modified, since NaOH etches 111 silicon too slowly. The etch for the experimental lots was performed in CP26 consisting of 5 parts HNO_3, 3 parts HF and 6 parts acetic acid. Because the verification lots were run using 100 silicon with a NaOH etch, a set of experiments were run to determine the comparative performance of 100-NaOH and 111-CP silicon solar cells. Table 3 summarizes the results of these runs. All the measurements are within two standard deviations except the red component of the current, which is statistically lower for the 111 cells. Because of the similarity in cell performance and the presence of a baseline control lot among the test wafers, only 100-NaOH etched wafers were used to make the control and monitor cells.

2.1.4 Monitor and Control Runs

To assure consistent cell processing and successful decontamination of the equipment, a monitor lot was run before

TABLE 3 COMPARISON OF 100 AND 111 CELL PERFORMANCE

Description	Isc mA	Voc mV	Pmax. mW	Imp mA	Vmp mV	Isc Blue mA	Isc Red mA
CP-111 Avg.	148.1	593.4	69.1	139.2	496.4	38.4	80.1
Ver. Lots Avg.	150.4	595.0	69.8	140.6	498.2	38.8	84.0
σ	1.48	2.09	.818	1.64	4.01	1.32	1.19
Coef. Var.	.01	.004	.012	.008	.034	.014	.009

each test lot and control silicon was run with the test wafers. The monitor and control lots have exhibited performance indistinguishable from the verification lots.

2.1.5 Decontamination Procedures

Cross-contamination of one impurity-containing group by another was prevented by proper cleaning and checked by the use of monitor lots. After one contaminated lot had been run, the diffusion and alloy tubes and boats were steam cleaned by gaseous HCl while in place at elevated temperatures. They were then cooled, removed from the furnace and etched in HF to remove the outer layer. In addition, all etchant and cleaning baths were changed with the containers being rinsed in deionized water. Between all steps the wafers or cells were cleaned in deionized rinsing systems with the conductivity of the water monitored.

After the cleaning process, a monitor lot was run using control silicon. No JPL impurity wafers were run until these monitor cells were completed and the test results showed no contamination of the equipment.

2.1.6 In-Line Quality Assurance

During cell processing,various quality control measure-

ments were performed. The required in-line measurements of cell parameters are listed below.

1. Thickness measurements were performed on etched wafers.
2. Resistivity measurements were taken on approximately 10% of each lot after etching.
3. Each run had the diffused sheet resistance measured on three control wafers, choosing a cell from the center and one from each edge of the diffusion tube. The center wafer was measured in five locations (wafer center and four equidistant points at a radial distance of one-inch from the wafer center).
4. Probe measurements of the sheet resistance of the front metal contracts after Ag plating were made for 10% of the cells in each lot. These values were correlated by means of optical measurements of contact thicknesses on sample cells.
5. Reflectance of a control wafer (having no metal pattern) was measured for every test run.

In addition to these in-line cell measurements, the following were recorded during processing:

- temperature of NaOH bath
- etch time
- temperature profile of diffusion tube

- diffusion time
- pressure during Al evaporation
- thickness of Al film
- temperature profile of alloy tube
- alloy time
- pressure during back evaporation
- spin and speed of photoresist spin-on
- bake time during photolithography
- bake temperature during photolithography
- exposure time
- development time
- pressure during front evaporation
- silver plating time
- pressure during AR coating
- monitor frequency shift during AR coating
- sinter time
- sinter temperature

While all of these values were measured, the rejection-acceptance criteria were restricted to those parameters that can adversely affect final cell performance. These in-line rejection-acceptance criteria are listed below.

1) Raw material for verification, monitor and control wafers shall be rejected if $\rho < 1.0$ ohm-cm or if $\rho > 3.0$ ohm-cm.

2) Etched thickness of verification, monitor, control and test wafers shall be between 10 and 12 mils.

3) A prediffusion profile of the furnace with tube in place shall show the active diffusion zone to be $870^{\circ}C \pm 5^{\circ}C$. The furnace heating element controls shall be adjusted to achieve this temperature.

4) The diffused sheet resistance of monitor runs and verification runs shall be $\geq 50\ \Omega/\square$ and $\leq 90\ \Omega/\square$. The diffused sheet resistance of control cells for test runs shall be $\geq 45\ \Omega/\square$ and $\leq 95\ \Omega/\square$.

5) The deposited thickness of aluminum metal shall be between 6,000 and 10,000 Å. A temperature profile of the diffusion tube made before formation of the p^+ layer shall show the active area to be $750^{\circ}C \pm 5^{\circ}C$. The furnace heating element controls shall be adjusted to achieve this temperature.

6) The deposited back contact shall be examined for adherence integrity. Areas of bubbling, delamination or bare silicon exceeding 1/2 sq. cm. on the wafer shall constitute rejection. If two wafers out of the run are rejectable, the run is rejected. A tape test is performed on a sample from each lot with metal lift-off constituting rejection of the lot. Rejected runs may have the contact metal removed and a fresh contact metal deposited. This

must be recorded on the lot follower, the QC log and brought to the attention of the program manager.

7) The photolithography inspection shall verify that the front metal contact pattern is free of resist areas and that the line width is correct to $\pm$ 25%.

8) The front contact pattern shall be inspected for severance, bubbling and delamination and a sample tape tested. If the major buss bars are severed (near the contact pads) or if a large number (>15) of the "fingers" are severed or missing, the cell is a reject. If three or more test cells are rejected or if less than ten control cells are accepted, or if the sample fails the tape test the run is rejected.

9) Plating thickness shall be a minimum of six microns. This will be measured by means of both a four point probe measurement and correlated with an optical measurement of the plating thickness. Either 10% of each lot or a minimum of 3 cells shall be measured. If any of these cells are underplated, the whole lot shall be checked and all underplated cells returned to the plating tank until the minimum acceptable thickness is reached.

2.2 Definition of Evaluation Parameters

Various cell parameters are measured on sample cells of

each lot in order to assure consistent processing and to provide additional information on cell behavior. The following sections describe the parameters which were used in the performance analysis including how they are measured and/or calculated and how they relate to physical mechanisms in the cell.

2.2.1 Absorption Efficiency

This value represents the fraction of incoming photons incident on the cell surface that actually enter the cell, as a function of wavelength.

The intensity of a reflected light beam is measured (versus wavelength) in an integrating sphere spectrophotometer with a Beckman DK-2 monochromator as the light source. The corrected reflectance represents the intensity ratio of the reflected beam to the incoming beam, thus normalizing for variations in the incoming light beam. Utilizing published data, the number of photons per unit area absorbed into the cell is computed for each 0.1 μ bandwidth between 0.4 μ to 1.0 μ. The ratio of the number of photons absorbed to the number of incoming photons, integrated for the six bandwidths, is the absorption efficiency.

This value is used to check the quality of the anti-reflector coating applied to the cell. Consistency of this parameter assures that the optical coupling to the cells is the same.

2.2.2 Quantum Yield

This value represents the ratio of carriers collected to the number of incoming photons per unit area as a function of wavelength.

A light beam is passed through a monochromator and alternately impinges on a defined unit area on the test solar cell and on a calibrated Eppley thermopile. The measured cell current is converted into the number of carriers collected. The current in the calibrated thermopile is used to find the number of incident photons. This ratio represents the cells efficiency of converting photons into carriers and collecting these carriers. Taking these measurements as a function of wavelength results in a curve of quantum efficiency over the bandwidth of solar radiation. The wavelength at which the maximum quantum efficiency occurs and the percent efficiency at this point are listed in the process evaluation table. An independent measurement of the shunt resistance enables one to correct for any internal shunting of carriers. However, other cell parameters such as short carrier lifetime and reflection of photons from the cell surface all contribute to a reduced quantum yield.

2.2.3 Carriers Collected per Absorbed Photon

No independent measurement is required as this parameter

equals the ratio of quantum yield to absorptivity summed over the entire solar spectrum. This ratio represents a modified quantum yield in that the effect of photon reflection is removed. Thus one measures the collection efficiency of the photons that enter the silicon.

2.2.4 Junction Capacitance

The junction capacitance is the capacitance across the depletion region of the junction. It is measured with a capacitance bridge using an ac signal with no dc voltage across the junction.

For lightly doped p-type bulk and a heavily doped n-type junction, the step-junction approximation is appropriate. The depletion region exists primarily on the p-side to a width adequate to ionize enough acceptors to equal the number of ionized donors in a very narrow segment of the heavily doped n-side. The width of the depletion layer is fixed by the voltage developed between the opposing two layers of charge; 1) the electrons on the p-side of the depletion layer and; 2) the holes on the n-side of the depletion layer.

The depletion region is in effect a parallel plate capacitor whose interplate spacing is proportional to the relative doping levels of the p- and n-sides.

2.2.5 Junction Conductance

This is a measurement of the cell leakage current and is read directly by the capacitance bridge as a resistance in parallel with the junction capacitor.

2.2.6 Series and Shunt Resistance

A solar cell is not a perfect diode. Each real cell has an effective resistance in series with the junction and a shunt resistance in parallel with the junction. The series resistance includes components from contact resistance in both the front and the back contacts, the resistance of the bulk silicon and the sheet resistance in the diffused region. The shunt resistance may be caused by surface leakage along the edge of the cell, by diffusion down dislocations or by metallization paths across the junction.

The idealized cell equation is given by

$$(1) \quad I = I_L - I_{01} \left(\exp\left(\frac{qV}{nkT} - 1\right)\right) - I_{02} \left(\exp\left(\frac{qV}{kT} - 1\right)\right)$$

where I = current collected from the cell

I_L = light generated current

I_{01} = reverse diode saturation current of space charge region

I_{02} = reverse diode saturation current of quasi-neutral region

$\frac{kT}{q}$ = thermal voltage

n = diode factor

V = voltage across the junction

If you take into account the series resistance and shunt resistance terms this equation becomes:

$$(2) \quad I + \frac{V+IRs}{Rsh} = I_L - I_{01}\ (\exp \frac{q}{nkT}\ (V-IRs) - 1) - I_{02}\ (\exp \frac{q}{kT}\ (V-IR) - 1)$$

where Rs = series resistance

Rsh = shunt resistance

The series resistance is derived from a comparison of two I-V curves for a cell at two distinct light levels, I_1 and I_2 where $I_2 \approx 2I_1$. A point is chosen on each I-V curve at an arbitrary level set 30 mA below the I_{SC} at each light level. The reciprocal slope of a straight line connecting these two points is the series resistance.

The shunt resistance is calculated by measuring the reverse current of the cell in the dark while maintaining 0.1 volt across the cell. The ratio of voltage to the current is then used as a measure of the shunt resistance. This is only an approximate value because the presence of a shunting diode may affect the measured current. However we are only using it as an indication of the junction quality so that a small value of this measured ratio indicates a problem in cell junction due to either a resistive or diode shunt.

2.2.7 Diode Factor and Reverse Saturation Current

The diode factor and the reverse diode saturation current can be obtained from either the static dark I-V characteristic or from the static I_{sc} - V_{oc} (photo-current versus photo-voltage) response to various levels of illumination. The current in both cases has two components-one originating from recombination within the space charge region-and the other from recombination in the quasi-neutral region.[3] The first exponential term in equation 2 is the component arising from the space charge region, with an effective diode factor of n and a diode saturation current of I_{01}. The second exponential term is the current component arising from the quasi-neutral regions with a diode factor of unity and a diode saturation current of I_{02}. The parameters I_{01}, I_{02} and n are determined using a method previously described in the literature[4,5,6].

The problem with this exact technique is the complicated relationship between the two diodes and the lack of any convenient parameter to determine in what regime the cell is actually operating. In other words, is the space charge diode or quasi-neutral diode dominating at the peak power point. To answer this question in simple manner, we have assumed the presence of only one diode operating at the maximum power point. The equation for I would then become:

$$(3) \quad I + \frac{V+IRs}{R_{sh}} = I_L - I_o \left(\exp \frac{q}{nkT} \quad (V-IRs) -1\right).$$

I_o and n are then calculated from the intercept and slope of the line drawn tangent to the I_{SC} vs V_{OC} curve at the voltage of maximum power. If the value of n is appreciably larger than 1, the space charge diode or a resistive shunt is affecting the cell peak power. Large values of I_o also indicate a lowering of the peak power due to diode or resistive shunting.

2.3 Data, Results and Analysis

The wafers supplied to Solarex by JPL were from ingots grown by the Westinghouse/Dow-Corning team under JPL Contract Number JPL-954331. Ingot number, growth process and impurity content information were withheld until completion of processing and evaluation of the experimental lots. Analysis in terms of the specific impurity content was finally performed and is included in this report. Table 4, Section 2.3.1, summarizes the identity and properties of the test wafers from data taken from the Phase II Summary and Eleventh Quarterly Report of the Westinghouse/Dow-Corning program, "Effect of Impurities and Processing on Silicon Solar Cells", written as part of the above referenced contract.

Every finished cell including all test, control, monitor and verification runs was measured to yield the following data taken at AMO and 25°C (standardized using a flight calibrated cell from NASA, Lewis):

- I-V curve
- I_{sc}
- I_{sc} blue with Corning Filter #9788
- I_{sc} red with Corning Filter #2408
- V_{oc}
- P_{max}
- I_{mp}
- V_{mp}

A summary of the performance of the experimental lots is given in Table 5, section 2.3.2. Table 6, section 2.3.3, shows these same performance data compared to the verification lots.

Additionally, the following measurements were performed on a sample basis, typically on at least one control cell and on one average performance test cell.

- reflection versus wavelength to assure proper AR coating and to factor the reflectivity dependence out of the spectral response data. A value for the absorption and the wavelength of minimum reflectance was noted

- quantum yield measurements
- dark I-V curve
- I_{sc} vs V_{oc} curve
- junction capacitance
- junction conductance
- series resistance
- diode factor n from I_{sc} vs V_{oc}
- I_o from I_{sc} vs V_{oc}

These test lot process evaluation data are shown in Table 7, section 2.3.4.

These measurements were performed to the degree necessary to understand the mechanisms at work in the cells. This means obtaining enough information to ascertain what fraction of degradation in output power is due to:

- loss in short-circuit current due to bulk degradation
- loss in open-circuit voltage due to junction degradation (n factor)
- loss in fill factor due to shunting by the impurities or due to an increase in I_o
- loss in fill factor due to series resistance.

A brief, lot-by-lot analysis follows in section 2.3.5 followed by a summary table of impurity content vs performance

for all of the experimental lots tested (Table 8, section 2.3.6). The spread in series resistance values indicated in Table 7 is process related, being approximately the same for both experimental and test cells. Seventy-eight percent of the series resistance values were within a mean value of 0.08 Ω ± 0.03 Ω.

It was deemed of particular interest to provide a comparison of the effect of doping levels on cell degradation for those impurities where sufficient lots were run. This is shown in a series of tables in section 2.3.7 for titanium, chromium, copper, tantalum, vanadium, carbon, iron, and manganese. The tabular data are presented not only as a comparison of impurity concentration level for the single impurity but also a comparison is indicated for the effects of multiple impurity additions.

TABLE 4

2.3.1 IDENTITY AND PROPERTIES OF TEST WAFERS

EXPERI-MENTAL LOT #	INGOT #	IMPURITY	BEST ESTIMATE OF CONCENTRATION (10^{15} ATOMS/CC)	BULK LIFETIME AS GROWN (uSEC)	BULK ESISTIVITY (Ω-CM)	NOTES
1	W-806	C	200-400	3.06	3.5-4.0	Polycry-stalline
2	W-087	Ca	?	2.81	3.4-3.8	
3	W-088	Cr	0.5	0.01	0.18-0.2	
4	W-089	Cu	2.0	2.37	0.19-0.21	
5	W-095	Mn	0.63	0.343	4.2-4.9	Fast Growth
6	W-094	Mn	1.0	0.38	2.8-4.2	Polycry-stalline
7	W-903	Mn	0.66	0.19	4.9-5.3	
8	W-092	P	28	7.83	1.7-5.6	Compensated
9	W-091	Cr-Mn	0.5/0.3	0.09	5.5-3.5	
10	W-090	Mn	0.7	0.06	0.21-0.2	
11	W-096S	Mn	0.63	0.34	4.6	Slow Growth
12	W-098	Mo	0.00092	1.4	3.6-4.3	
13	W-100	Cu/Ti	1.0/0.033	0.3	3.4-5.2	
14	W-102	Ti	0.11	0.21	3.8-6.4	Polycry-stalline
15	W-103	Ti	0.167	0.12	0.23-0.25	
16	W-128	Ta	<0.0008	2.62	4.5-3.7	
17	W-061	Cr/Ti	1.0/0.011	----	5.0-4.0	
18	W-066	Ti	0.033	0.49	6.0-3.9	
19	W-067	Cr/Mn/Ti	0.4/0.5/0.0033	----	5.5-5.2	
20	W-068	Cr	1.0	0.03	5.2-5.1	
21	W-104	Cu/Ti	2.0/0.14	0.16	3.8-4.2	Gross Lineage
22	W-105	V	0.4	0.07	0.23-0.26	Gross Lineage
23	W-109	C	<20-140	3.05	4.6-3.6	
24	W-110	Fe	0.8	---- †	0.16-0.15	
25	W-111	Cu/V	2.5/0.3	0.15	4.6-4.3	
26	W-074	Cr/Mn/Ni Ti/V	0.08/0.08/0.5 0.00033/0.0006	0.10	4.4	
27	W-073	Cr/Mn/Ni Ti/V	0.4/0.4/2.0 0.0024/0.004	0.09*	5.0-3.8	
28	W-072	Cr	0.4	0.06	5.0-4.5	
29	W-070	Al	100 (3.0)**	1.75	2.2-1.1	
30	W-069	Fe	1.0	0.04	5.8-5.0	Gross Lineage
31	W-112	Ta	<0.004	1.06	3.5-2.9	Gross Lineage
39	W-078	Base	---------	8.32	4.3-3.3	

* Measured after phosphorus diffusion

** Value based on resistivity measurement

† Insufficient electrical signal for measurement

2.3.2

TABLE 5
PERFORMANCE OF EXPERIMENTAL LOTS

Lot	Isc mA	Voc mV	Pmax mW	Imp mA	Vmp mV	Isc Blue mA	Isc Red mA	Fill Factor %
Verification 6 Lot AVG	150.4	595.0	69.8	140.6	498.2	38.8	84.0	78.3
E-1	143.5	573.3	60.8	128.5	472.5	36.3	80.5	73.8
E-2	144.2	578.2	64.7	134.5	480.8	40.5	76.3	77.6
E-3	134.2	610.1	59.3	114.8	515.9	37.0	71.4	72.4
E-4	138.9	606.5	64.0	125.5	510.0	38.2	72.9	76.0
E-5	134.6	561.2	57.6	121.8	472.0	37.9	69.5	76.3
E-6	130.7	548.3	53.7	119.7	448.3	35.3	68.6	74.9
E-7	133.1	559.3	57.9	122.8	470.8	36.0	71.3	77.8
E-8	143.4	593.5	66.6	132.8	502.7	31.5	83.9	77.5
E-9	107.6	516.6	40.4	93.4	431.4	36.4	48.5	72.7
E-10	135.9	607.7	61.0	117.8	516.3	37.9	71.7	73.9
E-11	138.2	562.9	59.7	125.9	475.8	37.2	73.2	76.7
E-12	131.7	545.5	56.4	123.0	458.3	35.9	69.5	78.5
E-13	93.9	517.8	36.7	85.8	426.3	34.8	37.3	75.5
E-14	83.0	478.6	26.2	65.4	397.0	28.2	35.8	66.0
E-15	66.8	535.5	21.6	46.5	466.2	21.5	30.5	60.4
E-16	134.8	565.0	54.8	118.8	460.0	36.3	69.8	72.0
E-17	104.0	518.6	42.2	96.1	439.6	37.4	42.9	78.2
E-18	98.2	520.1	38.8	90.9	426.9	35.9	39.2	76.0
E-19	122.8	539.2	51.0	112.0	455.0	38.8	57.3	77.0
E-20	128.3	539.9	53.7	118.3	452.9	38.5	62.3	77.5
E-21	86.9	492.9	32.3	79.0	409.3	35.9	29.7	75.4
E-22	85.5	562.3	34.9	74.3	472.0	36.2	29.6	72.6
E-23	147.2	576.1	67.1	139.0	483.8	37.4	78.1	79.1
E-24	131.8	612.0	59.8	116.1	515.6	39.4	66.0	74.1
E-25	91.4	495.4	33.9	82.2	415.0	31.3	36.8	74.9
E-26	134.6	560.7	58.4	125.0	465.6	35.8	68.5	77.4
E-27	113.9	526.6	47.0	106.5	491.3	37.7	47.8	78.4
E-28	144.5	567.0	62.2	131.5	473.1	37.5	75.2	77.5
E-29	112.7	556.5	48.7	102.9	468.8	34.9	53.8	77.6
E-30 * S	142.3	596.7	63.7	127.3	498.3	41.7	68.0	75.0
C	135.4	588.6	60.7	123.4	492.9	41.7	62.9	76.2
T	116.3	570.0	52.0	108.3	480.0	41.7	48.7	78.4
E-31	127.2	556.9	53.7	116.6	458.8	37.3	62.2	75.8
E-39	149.0	514.9	67.8	140.7	480.4	41.3	78.2	79.2

* Shows unusually sharp degradation from seed to tang end of crystal.

TABLE 6

2.3.3 PERFORMANCE OF EXPERIMENTAL LOTS COMPARED TO VERIFICATION LOTS

Lot	Isc Exp. / Isc Ver.	Voc Exp. / Voc Ver.	Pmax. Exp. / Pmax Ver.	Imp Exp. / Imp Ver.	Vmp Exp. / Vmp Ver.	Isc Blue Exp. / Isc Blue Ver.	Isc Red Exp. / Isc Red Ver.
E-1	0.95	0.96	0.87	0.91	0.95	0.94	0.96
E-2	0.96	0.97	0.93	0.96	0.97	1.04	0.91
E-3	0.89	1.03	0.85	.82	1.04	0.95	0.85
E-4	0.92	1.02	0.92	0.89	1.02	0.98	0.87
E-5	0.89	0.94	0.83	0.87	0.95	0.98	0.83
E-6	0.87	0.92	0.77	0.85	0.90	0.91	0.82
E-7	0.88	0.94	0.83	0.87	0.95	0.93	0.85
E-8	0.95	1.00	0.95	0.94	1.01	0.81	1.00
E-9	0.72	0.87	0.58	0.66	0.87	0.94	0.58
E-10	0.90	1.02	0.87	0.84	1.04	0.98	0.85
E-11	0.92	0.95	0.86	0.90	0.96	0.96	0.87
E-12	0.88	0.92	0.81	0.87	0.92	0.93	0.83
E-13	0.62	0.87	0.53	0.61	0.86	0.90	0.44
E-14	0.55	0.80	0.38	0.47	0.80	0.73	0.43
E-15	0.44	0.90	0.31	0.33	0.94	0.55	0.36
E-16	0.90	0.95	0.79	0.84	0.92	0.94	0.83
E-17	0.69	0.87	0.60	0.68	0.88	0.96	0.51
E-18	0.65	0.87	0.56	0.65	0.86	0.93	0.47
E-19	0.82	0.91	0.73	0.80	0.91	1.00	0.68
E-20	0.85	0.91	0.77	0.84	0.91	0.99	0.74
E-21	0.58	0.83	0.46	0.56	0.82	0.93	0.35
E-22	0.57	0.95	0.50	0.53	0.95	0.93	0.35
E-23	0.98	0.97	0.96	0.99	0.97	0.96	0.93
E-24	0.88	1.03	0.86	0.83	1.03	1.02	0.79
E-25	0.61	0.83	0.48	0.58	0.83	0.81	0.44
E-26	0.89	0.94	0.84	0.89	0.93	0.92	0.81
E-27	0.76	0.88	0.67	0.76	0.99	0.97	0.57
E-28	0.94	0.95	0.89	0.93	0.95	0.97	0.89
E-29	0.75	0.93	0.70	0.73	0.94	0.90	0.64
E-30	S 0.95 C 0.90 T 0.77	1.00 0.99 0.96	0.91 0.87 0.74	0.91 0.87 0.77	1.00 0.99 0.96	1.07 1.07 1.07	0.81 0.75 0.56
E-31	0.84	0.94	0.77	0.83	0.92	0.96	0.74
E-39	0.99	0.97	0.97	1.00	0.96	1.06	0.93

TABLE 7

2.3.4

TEST LOT PROCESS EVALUATION

Lot	P_{max} mW	Absorption Efficiency %	Quantum Yield λ max. μ	% Q Y atλmax	Carriers Collected Per Absb. Photon	Junction Cap. μF	Junction Cond. M℧	R_{series} Ω Avg.	R_{shunt} Ω Median	Diode Factor	I_o mA (10^{-8})
Verification Lot AVG.	69.8	91	0.62	91	0.83	0.111	0.72	0.079	5,000	1.05	3.78
E-1 Control (100)	69.6	91	0.65	83	0.83	0.111	0.10	0.083	7,140	1.03	3.0
E-1 Test E-1 Test	60.7	88	0.65	85	0.79	0.063	1.43	0.19	450	1.47	1000.
E-2 Control (100)	68.6	91	0.60	89	0.82	0.107	0.01	0.115	9,000	1.02	3.2
E-2 Test	64.3	87	0.65	87	0.85	0.086	0.40	0.092	1,200	1.05	9.3
E-3 Control (100)	68.9	91	0.65	91	0.84	0.106	0.04	0.048	10,636	1.01	2.0
E-3 Test	59.3	88	0.65	84	0.77	0.344	11.86	0.040	295	1.42	2000.
E-4 Control (100)	69.4	90	0.65	85	0.80	0.103	0.07	0.057	1,481	1.08	9.0
E-4 Test	64.0	89	0.60	83	0.79	0.341	0.71	0.120	184	1.18	8.0
E-5 Control (100)	69.3	94	0.65	92	0.86	0.103	0.13	0.081	3,255	1.11	9.0
E-5 Test	55.3	88	0.60	87	0.78	0.082	4.44	0.091	246	1.13	40.

2.3.4

TABLE 7 (Continued)

TEST LOT PROCESS EVALUATION

Lot	P_{max} mW	Absorption Efficiency %	Quantum Yield λ max. μ	% Q Y at λ max	Carriers Collected Per Absb. Photon	Junction Cap. μF	Junction Cond. M℧	R_{series} Ω Avg.	P_{shunt} Ω Median	Diode Factor	I_o mA (10^{-8})
E-6 Control	70.6	90	0.65	90	0.84	0.107	1.83	0.073	1,360	1.03	3.26
E-6 Test	53.7	91	0.60	84	0.72	0.085	1.05	0.113	1,070	1.17	185
E-7 Control	70.3	92	0.65	90	0.84	0.108	0.13	0.075	13,200	1.04	5.00
E-7 Test	57.9	92	0.65	87	0.70	0.068	0.88	0.094	750	1.06	18.5
E-8 Control	69.3	91	0.70	91	0.81	0.111	0.44	0.069	4,410	1.09	10.0
E-8 Test	66.6	89	0.75	86	0.80	0.120	0.68	0.079	2,640	1.05	4.12
E-9 Control	71.8	91	0.65	93	0.85	0.107	0.19	0.062	3,070	1.13	223
E-9 Test	40.4	91	0.60	31	0.24	0.082	2.82	0.061	275	1.13	154
E-10 Control	70.4	92	0.65	91	0.83	0.108	0.22	0.070	7,020	1.13	23.4
E-10 Test	61.0	93	0.64	83	0.72	0.335	409	0.063	711	1.20	49.5
E-11 Control	69.5	93	0.65	92	0.84	0.109	1.22	0.059	5,571	1.13	20.9

2.3.4

TABLE 7 (Continued)

TEST LOT PROCESS EVALUATION

Lot	P_{max} mW	Absorption Efficiency %	Quantum Yield λ max. μ	Quantum Yield % Q Y at λ max	Carriers Collected Per Absb. Photon	Junction Cap. μF	Junction Cond. M℧	R_{series} Ω Avg.	R_{shunt} Ω Median	Diode Factor	I_o mA (10^{-8})
E-11 Test	59.7	92	0.65	88	0.78	0.081	10.4	0.09	131	1.12	42.5
E-12 Control	69.2	91	0.70	90	0.80	0.105	0.15	0.061	6,654	1.12	24.6
E-12 Test	56.4	93	0.65	89	0.76	0.077	3.25	0.053	810	1.07	34.5
E-13 Control	70.0	92	0.65	92	0.84	0.103	1.08	0.033	62,700	1.10	12.5
E-13 Test	36.7	92	0.57	76	0.48	0.085	1.44	0.051	9,788	1.20	706
E-14 Control	70.9	92	0.65	91	0.84	0.111	3.0	0.054	3,320	1.10	11.1
E-14 Test	26.2	92	0.55	75	0.45	0.083	4.98	0.092	243	1.63	33,600
E-15 Control	69.9	91	0.65	91	0.86	0.100	0.46	0.041	3,690	1.12	25.1
E-15 Test	21.6	91	0.55	60	0.39	0.33	14.0	0.052	70	1.83	34,900
E-16 Control	69.5	91	0.63	91	0.87	0.098	0.044	0.081	47,000	1.03	2.4
E-16 Test	54.8	91	0.65	87	0.80	0.079	4.34	0.17	6,630	1.17	84

TABLE 7 (Continued)

2.3.4

TEST LOT PROCESS EVALUATION

Lot	P_{max} mW	Absorption Efficiency %	Quantum Yield λ max. μ	% Q Y at λ max	Carriers Collected Per Absb. Photon	Junction Cap. μF	Junction Cond. M℧	R_{series} Ω Avg.	R_{shunt} Ω Median	Diode Factor	I_o mA (10^{-8})
E-17 Control	69.6	91	0.62	91	0.85	0.100	0.17	0.066	18,450	1.05	5.2
E-17 Test	42.2	91	0.56	83	0.58	0.08	0.58	0.071	3,110	1.21	690
E-18 Control	69.3	91	0.63	90	0.86	0.096	3.35	0.091	10,430	1.05	9.3
E-18 Test	38.8	91	0.57	80	0.55	0.081	0.23	0.09	6,860	1.35	2900
E-19 Control	68.9	91	0.65	91	0.87	0.097	0.49	0.1	5,670	1.28	18.6
E-19 Test	51.0	91	0.60	87	0.71	0.081	2.94	0.07	1,430	1.32	1980
E-20 Control	70.8	91	0.62	91	0.85	0.108	0.54	0.101	6,240	1.04	4.8
E-20 Test	53.7	91	0.62	88	0.75	0.081	2.25	0.088	1,390	1.2	260
E-21 Control	70.2	91	0.65	95	0.88	0.103	1.19	0.097	8,140	1.11	20
E-21 Test	32.3	91	0.54	79	0.50	0.08	0.13	0.078	6,200	1.32	4,700
E-22 Control	69.1	91	0.62	84	0.81	0.107	0.70	0.085	4,580	1.07	8.2

2.3.4

TABLE 7 (Continued)

TEST LOT PROCESS EVALUATION

Lot	P_{max} mW	Absorption Efficiency %	Quantum Yield λ max. µ	% Q Y at λ max	Carriers Collected Per Absb. Photon	Junction Cap. µF	Junction Cond. M℧	R_{series} Ω Avg.	R_{shunt} Ω Median	Diode Factor	Io mA (10^{-8})
E-22 Test	34.9	91	0.54	74	0.48	0.331	3.2	0.068	430	1.41	1,700
E-23 Control	70.4	91	0.65	98	0.90	0.106	0.51	0.109	3,030	1.08	10
E-23 Test	67.1	91	0.66	93	0.88	0.079	0.64	0.086	16,100	1.05	9.1
E-24 Control	71.6	90	0.60	93	0.88	0.110	0.18	0.075	39,000	1.07	7.8
E-24 Test	59.8	90	0.60	89	0.79	0.385	5.8	0.074	859	1.22	52.5
E-25 Control	70.2	90	0.65	92	0.87	0.105	0.5	0.089	8,372	1.08	11
E-25 Test	33.9	91	0.57	66	0.45	0.081	3.4	0.078	565	1.06	110
E-26 Control	68.3	91	0.67	89	0.82	0.110	1.85	0.122	1,685	1.11	17.7
E-26 Test	58.4	91	0.70	71	0.60	0.080	0.49	0.086	2,977	1.24	314.6
E-27 Control	70.8	90	0.61	95	0.93	0.110	0.78	0.094	15,569	1.15	38.6
E-27 Test	47.0	91	0.56	85	0.66	0.080	2.19	0.069	542	1.14	225

TABLE 7 (Continued)

2.3.4

TEST LOT PROCESS EVALUATION

Lot	P_{max} mW	Absorption Efficiency %	Quantum Yield λ max. μ	Quantum Yield % Q Y at λ max	Carriers Collected Per Absb. Photon	Junction Cap. µF	Junction Cond. M℧	R_{series} Ω Avg.	R_{shunt} Ω Median	Diode Factor	Io mA (10^{-8})
E-28 Control	69.4	91	0.67	88	0.84	0.110	1.30	0.129	11,408	1.10	14.4
E-28 Test	62.2	90	0.65	89	0.82	0.080	0.57	0.113	2,756	1.19	149
E-29 Control	70.4	91	0.65	94	0.89	0.100	0.72	0.124	6,102	1.19	70.1
E-29 Test	48.7	90	0.62	86	0.69	0.130	1.71	0.120	2,468	1.23	334
E-30 Control	72.2	91	0.63	94	0.86	0.107	0.97	0.096	15,391	1.07	9.43
E-30 Test	63.7 60.7 52.0	91	0.63	88	0.75	0.201	3.04	0.058	864	1.23	148
E-31 Control	65.4	91	0.68	94	0.87	0.108	1.61	0.103	4,347	1.12	24.4
E-31 Test	53.7	90	0.63	90	0.79	0.087	1.13	0.058	2,313	1.48	6510
E-39 Control	69.6	91	0.60	92	0.89	0.110	0.74	0.098	11,594	1.08	8200
E-39 Test	67.8	91	0.65	92	0.88	0.080	1.26	0.056	5,024	1.01	3800

2.3.5 Lot-by-Lot Performance Analysis

E - 1 There is a decrease in open-circuit voltage due in part to a slightly higher bulk resistivity than the verification cells. The blue current is not statistically different from the verification lots. The major degradation is in the bulk or red current, indicating a decrease in bulk lifetime. Also there is a decrease in fill factor due to resistive and diode shunting suggesting the presence of a high concentration of carbon near the junction.

E - 2 This lot exhibits a decrease in open circuit voltage mainly due to a higher bulk resistivity. There was also a higher blue current component than the verification lots. Once again the major degradation occurred for the bulk red current, again indicating a decrease in bulk lifetime. The fill factor of lot E-2 is nearly equal to the average of the verification lots. The junction diode is well behaved for these test cells, being indistinguishable from the verification cell diodes. Therefore it appears that calcium does not degrade junction performance.

E - 3 The lot exhibited a significantly higher open circuit voltage that was almost entirely attributable to the lower bulk resistivity. This lot also exhibited a lower short circuit current and red response indicating some degradation of the bulk lifetime probably due to the presence of chromium. The blue current is slightly less on the test cells. Finally the test cells exhibited lower fill factors due to both resistive and diode shunting.

E - 4 E-4 exhibited a higher open circuit voltage and lower current attributable to the lower bulk resistivity of the test wafers. Indeed when the effect of the covariates is factored out, there appears to be no statistical difference between the maximum power of the test cells and the maximum power of the verification cells. Correspondingly, the fill factor is also nearly the same. At this level of doping the copper does not appreciably affect the cell performance.

E - 5 This lot exhibits a lower open circuit voltage than the verification cells. This is partially due to a higher bulk resistivity. The major

degradation is due to red or bulk current. This loss in current is due to a decrease in bulk lifetime caused by the manganese. The fill factor of this lot is nearly as high as for the verification lots, however several cells show appreciable resistive shunts, while the majority have excellent diode characteristics. Since none of the monitor or control cells have shown this shunting, we feel it is a result of impurity level. At present we do not know why it occurs in some but not all cells.

E - 6 The electrical performance measurements are based on the three test cells that were not severely shunted. The decrease in voltage is due in part to a slightly higher bulk resistivity than the verification lot, but this does not explain all of the voltage degradation. The blue current shows very little variation from the verification lots. The major degradation is in the bulk or red current, indicating a probable decrease in bulk lifetime due to the incorporated manganese. The fill factor is also somewhat reduced even in these cells, indicating shunting is a problem in the best cells from this lot.

E - 7 The decrease in open-circuit voltage is almost entirely due to the higher bulk resistivity. While the average fill factor was nearly equal to the control cells, several test cells did show significant shunting. Once again, the blue current is normal but the red or bulk current is degraded, indicating again the probable decrease in bulk lifetime due to the incorporated manganese.

E - 8 This lot exhibited only minor degradation in power with most of the loss due to a decrease in blue response. The incorporated phosphorous has very little effect on the bulk and the junction itself, but does seem to affect the front surface behavior of the cell.

E - 9 The electrical performance decreased for all components except the blue current. A large decrease in red or bulk current probably results from a degradation in bulk lifetime. As usually appears to be the case for Mn, several cells are shunted while the remainder have excellent fill factors. Having previously processed both Mn and Cr incorporated cells, we can compare the results of single and multiple doping.

Lot #5 Mn 0.63 $\cdot 10^{15}$ at/cc P/Po = 0.83

Lot #3 Cr 0.5 $\cdot 10^{15}$ at/cc P/Po = 0.85

P/Po (Lot #5) x P/Po (Lot #3) - 0.71

Lot E-9 had 0.5 x 10^{15} atoms/cc of Cr and 0.3 x 10^{15} atoms/cc of Mn and had P/Po = 0.58. This lot, therefore, exhibits a synergistic effect with the multiple doping of Mn and Cr resulting in a more severe degradation than the sum of the two degradations alone.

E - 10 The higher open-circuit voltage is consistent with the lower bulk resistivity. Once again, the blue current is unchanged. The red current is somewhat degraded, indicating a reduced bulk lifetime and the fill factor varies with many cells having normal fills and several showing shunts. The mechanisms for degradation appear to be the same as for other Mn containing lots.

E - 11 The lower voltage is consistent with the higher bulk resistivity. The blue current is similar to that of control cells. The fill factor is somewhat reduced with some cells showing a great deal of shunting and others having very high fill

factors. As previously, the greatest degradation caused by Mn is in the red or bulk current, probably due to a reduced bulk lifetime.

E - 12 The open circuit voltage is somewhat lower than would be expected for this bulk resistivity range. The blue current and fill factor are nearly identical to that of the control silicon cells. The red or bulk current is reduced, indicating a probable reduction in bulk lifetime due to the presence of the molybdenum.

E - 13 This lot exhibited severe degradation of all components except the blue current and fill factor, which are nearly consistent with control silicon values. The red or bulk current suffered severe degradation, indicating that the Cu/Ti mixture probably severely degraded the bulk lifetime. The open circuit voltage decreased much more than would be expected by the higher resistivity. This Cu/Ti lot degraded slightly more than Lot E-18 which contained exactly the same amount of titanium but no copper. Indeed, Lot E-13 exhibited slightly lower current, voltage and power than Lot E-18, so in this lot the additional copper caused a slight loss of power.

E - 14 This lot contained polycrystalline wafers with many of the cells exhibiting severe shunts. The cells without shunting were tabulated in the tables, indicating that even without shunting the cells exhibit a greater than 50% loss of power. All components are reduced, including blue current, red or bulk current and voltage. The concentration of titanium in those cells is sufficient to cause bulk, junction and surface problems.

E - 15 This lot exhibited severe degradation. The open-circuit voltage was higher than for Lot E-14, as would be expected because of the lower bulk resistivity. Even though there were no apparent grain boundaries in these samples, many of the cells were badly shunted, indicating that it may have been the titanium rather than the grain boundaries causing the shunting in Lot E-14. This concentration of titanium is sufficient to degrade the cells to less than 1/3 the power using control silicon, with severe degradation of all components exhibited.

E - 16 The open-circuit voltage of this lot is consistent with the higher bulk resistivity. There is no apparent degradation of blue current but several

cells showed lower fill factors that appeared to be a result of some shunting. The major power loss was a result of reduced red or bulk current, indicating that the tantalum probably reduces the bulk lifetime.

E - 17 The voltage was significantly lower than would be expected for the higher bulk resistivity. The blue current was not degraded and the fill factors were equal to that for control cells. The major loss was in red or bulk current, indicating a probable reduction in bulk lifetime. A comparison of this lot with other chrome and titanium lots indicates that while a large concentration of titanium affects the blue current and fill factor a smaller amount in combination with chrome does not. However, this lot indicates that the two together do not produce more degradation than would be expected from the sum of the two separate degradations.

E - 18 The voltage was lower than expected for the higher resistivity. There was no apparent shunting confirming the observation that a small amount of Ti does not shunt the cells, while Lots 14 and 15 indicated that a larger concentration

of Ti does. Once again, the major loss of power was due to bulk current loss, although the blue current was lower than for control silicon.

E - 19 The cells exhibit open-circuit voltages slightly lower than would be expected for this bulk resistivity. The blue current is almost identical to that for control silicon cells. Most of the cells had normal fill factors, although several exhibited minor shunting behavior. The bulk current is the major area of degradation, indicating a reduction in bulk lifetime. The amount of degradation appears to be consistent with that expected from the sum of the three individual degradations, Cr/Mn/Ti.

E - 20 There was moderate to severe shunting on some cells. The IV characteristics also showed a high excess junction current compared to the control cells. It is interesting to compare the reduced red response with Lot E-3 which contained half the concentration of Cr:

	Control	E-3	E-5
RED I_{SC}(mA)	84	71.4	62.3

The degradation is directly proportional to the concentration level, which is strong evidence of bulk lifetime degradation due to Cr. The maximum output power was decreased to about 75 percent in Lot E-20 for the indicated concentration of Cr. Fill factor was good as was also blue response. The values of V_{OC} are consistant with starting resistivity, ie.:

Lot #	ρ (Ωcm)	V_{OC}(mV)
E- 3	0.18-0.2	610
E-20	5.2-5.1	540

E - 21 There was a very severe reduction in red response (less than the blue response). The impurities in this lot were Cu-Ti and in comparison with other runs containing only Cu it may be concluded that Ti is the principal cause of the performance deterioration. A similar degradation was experienced on Lot E-13 which also contained Cu-Ti with a somewhat lower concentration of Ti. The degradation in Lot E-13, though not as severe as in Lot E-21, was still excessive. Lot E-21 exhibited over 50 percent loss in output power compared to the verification runs. There was little or

no evidence of shunting in the cells. Some etch defects were observed in the test wafers, which goes along with the presence of gross lineage as reported in the Westinghouse/Dow-Corning data for this ingot.

E - 22 There is an inconsistency in the reported resistivity, 0.23-0.26 Ωcm, as compared to the as-measured value of 1.8-3.1 Ωcm. The measured value for V_{OC} = 560 mV seems more consistent with the higher measured value. This lot exhibited gross lineage and was grown with vanadium contamination. The output power was down by about half of the control value with a very severely degraded red response indicating heavy losses in bulk current due to the presence of V. There was also moderate to severe shunting in evidence on all the test cells. The I_{SC} vs V_{OC} characteristics exhibited a lot of excess junction current; the diode n-factor was high with n = 1.41. The blue response was a little less than the control and the FF was about 73 percent as compared to 78 percent for the control.

E - 23 This lot was carbon doped with an estimated concentration <20-140 x 10^{15} atoms/cc. It displayed rather good characteristics being almost indistinguishable from the control wafers for all the measured parameters.

E - 24 There was very severe shunting on all the test cells; FF was ∿74 percent. Open-circuit voltage was relatively high, 612mV, consistent with the lower resistivity (0.15-0.17 Ωcm). Overall degradation was moderate with average $P_m \simeq 60$ mW as compared to ∿70 mW for the control. Red response was lowered (∿66 mA compared to 80 mA for the control). Blue response was the same as for the control. This lot contained 0.8 x 10^{15} atoms/cc Fe.

E - 25 Vanadium in combination with Cu results in similar performance degradation as Cu-Ti (e.g. Lot E-21). The maximum output power was reduced to about half as was also the red response indicating a loss in bulk current due to lifetime degradation. There was severe shunting on most of the test cells.

E - 26 The wafers in this lot came from a multiply doped ingot (Cr/Mn/Ni/Ti/V). Perhaps due to relatively

light doping or perhaps to synergistic effects, the performance degradation was not as severe as might have been expected from some of the contaminants (e.g. Ti or V). FF was good and equal to 77 percent. Output power was reduced to 84 percent of the control wafer value. The test I-V's look normal with some shunting existing for wafers from the tang end of the ingot. The I_{sc} vs. V_{oc} curve was very much the same for both the test and control wafers.

E - 27 This was a multiply doped ingot with the same five impurities as in E-26, however, at a somewhat higher doping concentration level. This was reflected in reduced performance compared to E-26 as summarized below:

Lot #	P/P_o	$\frac{I_{sc}}{I_{sco}}$	$\frac{V_{oc}}{V_{oco}}$
26	0.84	0.89	0.94
27	0.67	0.76	0.88

The tabulated values are referred to the verification run values. The reduced $\bar{V}_{oc}$ for run E-27 compared to E-26 is probably due to increased concentration of impurities in E-27 since both runs had about the same starting resistivity. Performance degradation was still not as bad as for some of the

constituent impurities taken individually (e.g. V or Ti, see E-15 and E-22). The IV characteristics for all the test cells were all quite uniform. Blue response was almost the same as for the control lot. The I_{sc} vs V_{oc} curves for the control and test wafers were almost identical except for a lower V_{oc} for the test wafers by about 60 mV.

E - 28 Performance in this Cr doped lot was very close to the control wafers indicating that the presence of Cr in the reported concentration level of 0.4×10^{15} atoms/cc is not deleterious. There was about a 20mV lower value of V_{oc} for the test wafers, but this is consistent with the higher value of starting resistivity as compared to the control group. The I_{sc} vs V_{oc} curves showed low excess current for both the control and test wafers; n-factor was about 1.1 for both groups.

E - 29 This lot was contaminated with 10^{17} atoms/cc aluminum. There was severe shunting on some of the test cells. Overall characteristics were degraded including both red and blue response.

The maximum output power was down to 70 percent of the control wafers value. Fill factor was good (∿78 percent). The I_{SC} vs V_{OC} curves were similar for both control and test (control n-factor = 1.19, test n-factor = 1.23). Saturation current, I_O, was higher by an order of magnitude for the test group. Open-circuit voltage was lower for the Al doped wafers even though the starting resistivity was nearly the same as the control group.

E - 30 This was an iron contaminated ingot with Fe concentration about 20 percent higher than the Fe contaminated crystal of run E-24. Unlike that ingot, however, this one was of higher resistivity, 5.8-5.0 Ωcm compared to 0.16-0.15 Ωcm. This was reflected in the higher value of V_{OC} for E-24, 0.612 volts. The ingot for E-30 was noted as exhibiting gross lineage. We found a distinct gradient of degradation on this test run from seed to tang end of the crystal, so much so that we calculated three separate averages for the performance parameters (see, for example, Table 5 and 6). There were moderate shunting

effects on the test wafers closer to the seed end of the crystal but overall performance was not too badly degraded until about the center of the ingot and got progressively worse for the wafers toward the tang end of the crystal. A performance summary is as follows:

	$\frac{P}{P_o}$	$\frac{I_{sc}}{I_{sco}}$	$\frac{V_{oc}}{V_{oco}}$	FF
S	0.91	0.95	1.00	.75
C	0.87	0.90	0.99	.76
T	0.74	0.77	0.96	.78

The blue response was the same for all the test cells and just a little lower than the controls; the red response degraded from an I_{sc} value of $\sim$68 mA at the seed end to $\sim$48 mA near the tang end indicating losses in bulk current. The I_{sc} vs V_{oc} characteristics of the test wafer indicated an n-factor of 1.23 and $I_o = 1.48 \times 10^{-9}$A for a sample taken near the center of the ingot. It indicated more excess junction current near the maximum power point than the control.

E - 31 This ingot had a very small reported concentration of Ta ($<0.004 \times 10^{15}$ atoms/cc). It was rather severely degraded in performance with maximum output power down to about 77 percent of the control value. There was an indicated note of gross lineage for this ingot. Resistivity range was close to the control wafers but V_{oc} was down to about 94 percent of the control. Blue response was the same as the control, and red response was down to about 80 percent of the control. Fill Factor was about 76 percent for the test units. The I_{sc} vs V_{oc} characteristic for the test piece showed a n-factor value = 1.48 with evidence of high excess junction current at about 300 mV.

E - 39 This lot was an uncontaminated baseline ingot with a resistivity of 3.5-4.4 Ωcm. Its performance was quite close to the control wafers in all respects with a FF = 79.2 percent. Following is a summary performance comparison:

$\frac{I_{sc}}{I_{sco}}$	$\frac{V_{oc}}{V_{oco}}$	$\frac{I_{sc\ red}}{I_{sco}}$	$\frac{I_{sc\ blue}}{I_{sco}}$	$\frac{P_m}{P_{mo}}$
$\frac{149}{149}$	$\frac{575}{588}$	$\frac{78}{77}$	$\frac{41}{42}$	$\frac{68}{69.6}$

TABLE 8

2.3.6 IMPURITY CONTENT VS PERFORMANCE

EXPERIMENTAL LOT #	IMPURITY	CONCENTRATION* 10^{15} ATOMS/CC	P/P_0	$\frac{I_{SC}}{I_{SCO}}$	$\frac{V_{OC}}{V_{OCO}}$	FF
1	C	200-400	0.87	0.95	0.96	74
2	Ca	?	0.93	0.96	0.97	78
3	Cr	0.5	0.85	0.89	1.03	72
4	Cu	2.0	0.92	0.92	1.02	76
5	Mn	0.63	0.83	0.89	0.94	76
6	Mn	1.0	0.77	0.87	0.92	75
7	Mn	0.66	0.83	0.88	0.94	78
8	P	28	0.95	0.95	1.00	78
9	Cr-Mn	0.5/0.3	0.58	0.72	0.87	73
10	Mn	0.7	0.87	0.90	1.02	74
11	Mn	0.63	0.86	0.92	0.95	77
12	Mo	0.00092	0.81	0.88	0.92	79
13	Cu/Ti	1.0/0.033	0.53	0.62	0.87	76
14	Ti	0.11	0.38	0.55	0.80	66
15	Ti	0.167	0.31	0.44	0.90	60
16	Ta	<0.0008	0.79	0.90	0.95	72
17	Cr/Ti	1.0/0.011	0.60	0.69	0.87	78
18	Ti	0.033	0.56	0.65	0.87	76
19	Cr/Mn/Ti	0.4/0.5/0.0033	0.73	0.82	0.91	77
20	Cr	1.0	0.77	0.85	0.91	77
21	Cu/Ti	2.0/0.14	0.46	0.58	0.83	7[illegible]
22	V	0.4	0.50	0.57	0.95	73
23	C	<20-140	0.96	0.98	0.97	79
24	Fe	0.8 †	0.86	0.88	1.03	74
25	Cu/V	2.5/0.3	0.48	0.61	0.83	75
26	Cr/Mn/Ni Ti/V	0.08/0.08/0.5 0.00033/0.0006	0.84	0.89	0.94	77
27	Cr/Mn/Ni Ti/V	0.4/0.4/2.0 0.0024/0.004	0.67	0.76	0.88	78
28	Cr	0.4	0.89	0.94	0.95	77
29	Al	100 (3.0)**	0.70	0.75	0.93	78
30	Fe	1.0	0.91S 0.87C 0.74T	0.95 0.90 0.77	1.00 0.99 0.96	75 76 78
31	Ta	<0.004	0.77	0.84	0.94	76
39	Base	---------	0.97	0.99	0.97	79

* Data from Ref. 7
** Value based on resistivity measurement
† Lifetime in ingot could not be determined due to insufficient signal

TABLE 9

2.3.7 Summary of Titanium Impurity Runs

Lot #	Concentration 10^{15} Atoms/cc	$\frac{P}{P_O}$	$\frac{I_{sc}}{I_{sco}}$	$\frac{V_{oc}}{V_{oco}}$	Resistivity (Ωcm)
Ti					
14	0.11	0.38	0.55	0.80	3.8-6.4 Poly-crystalline
15	0.167	0.31	0.44	0.90	0.23-0.25
18	0.033	0.56	0.65	0.87	6.0-3.9
Cu-Ti					
13	1.0/0.033	0.53	0.62	0.87	3.4-5.2
21	2.0/0.14	0.46	0.58	0.83	3.8-4.2 Gross Lineage
Cr-Ti					
17	1.0/0.011	0.60	0.69	0.87	5.0-4.0
Cr-Mn-Ni Ti-V					
26	0.08/0.08/0.5 0.00033/0.0006	0.84	0.89	0.94	4.4
27	0.4/0.4/2.0 0.0024/0.004	0.67	0.76	0.88	5.0-3.8

NOTES: Performance is severely degraded with the presence of Ti. Complicated interactions in lots 26 and 27 result in some compensating effects; however, the Ti concentration is much reduced in these two lots compared to the other lots indicated in the table. Lot 21 contained a level of Ti similar to that contained in lot 15 (1.4×10^{14} vs. 1.67×10^{14}), but the former had also incorporated 2×10^{15} Cu as well. On the other hand, lot 21 had a P/P_O ratio of 0.46 as opposed to the ratio of only 0.31 for lot 15. In this case there may have been a significant positive synergistic effect. This may be contrasted with the results of lot 13 vs. lot 18 with identical Ti levels, but with the addition of 1×10^{15} Cu in the former. In this case the P/P_O ratio was slightly worse for the Cu-containing cells than for the non-Cu-containing cells (0.53 and 0.56 respectively), indicating no (or perhaps negative) benefit to the addition of Cu. Note also that the concentration of Ti was lower in lot 13 as compared to lot 21.

TABLE 10

2.3.7 Summary of Chromium Impurity Runs

Lot #	Concentration 10^{15} Atoms/cc	$\frac{P}{P_o}$	$\frac{I_{sc}}{I_{sco}}$	$\frac{V_{oc}}{V_{oco}}$	Resistivity (Ωcm)
Cr					
3	0.5	0.85	0.89	1.03	0.18-0.2
20	1.0	0.77	0.85	0.91	5.2-5.1
28	0.4	0.89	0.94	0.95	5.0-4.5
Cr-Mn					
9	0.5/0.3	0.58	0.72	0.87	5.5-3.5
Cr-Ti					
17	1.0/0.011	0.60	0.69	0.87	5.0-4.0
Cr-Mn-Ti					
19	0.4/0.5/0.0033	0.73	0.82	0.91	5.5-5.2
Cr-Mn-Ni Ti-V					
26	0.08/0.08/0.5 0.00033/0.0006	0.84	0.89	0.94	4.4
27	0.4/0.4/2.0 0.0024/0.004	0.67	0.76	0.88	5.0-3.8

NOTES: There is some concentration related degradation with Cr which is also severely affected with the simultaneous presence of Mn or Ti; some evidence that the presence of Ni may compensate somewhat the presence of smaller concentrations of Mn and Ti.

TABLE 11

2.3.7 Summary of Copper Impurity Runs

Lot #	Concentration 10^{15} Atoms/cc	$\frac{P}{P_o}$	$\frac{I_{sc}}{I_{sco}}$	$\frac{V_{oc}}{V_{oco}}$	Resistivity (Ωcm)
Cu					
4	2.0	0.92	0.92	1.02	0.19-0.21
Cu-Ti					
13	1.0/0.033	0.53	0.62	0.87	3.4-5.2
21	2.0/0.14	0.46	0.58	0.83	3.8-4.2 Gross Lineage
Cu-V					
25	2.5/0.3	0.48	0.61	0.83	4.6-4.3

NOTE: The presence of copper in the concentration range indicated does not appear to be particularly deleterious; small additions of Ti or V severely degrade performance (less than 50 percent maximum output power).

TABLE 12

Summary of Tantalum Impurity Runs

Lot #	Concentration 10^{15} Atoms/cc	$\frac{P}{P_o}$	$\frac{I_{sc}}{I_{sco}}$	$\frac{V_{oc}}{V_{oco}}$	Resistivity (Ωcm)
Ta					
16	<0.0008	0.79	0.90	0.95	4.5-3.7
31	<0.004	0.77	0.84	0.94	3.5-2.9 Gross lineage

NOTES: Extremely small concentrations of Ta severely degrade solar cell performance based on these two sample lots.

TABLE 13

2.3.7 Summary of Vanadium Impurity Runs

Lot #	Concentration 10^{15} Atoms/cc	$\frac{P}{P_o}$	$\frac{I_{sc}}{I_{sco}}$	$\frac{V_{oc}}{V_{oco}}$	Resistivity (Ωcm)
V					
22	0.4	0.50	0.57	0.95	0.23-0.26 Gross Lineage
Cu-V					
25	2.5/0.3	0.48	0.61	0.83	4.6-4.3
Cr-Mn-Ni Ti-V					
26	0.08/0.08/0.5 0.00033/0.0006	0.84	0.89	0.94	4.4
27	0.4/0.4/2.0 0.0024/0.004	0.67	0.76	0.88	5.0-3.8

NOTES: No apparent correlation with ingot resistivity except for higher Voc in lot #22 which is lower resistivity; vanadium appears to severely degrade performance except in the very small concentrations as indicated for lots #26 and #27.

TABLE 14

2.3.7 Summary of Carbon Impurity Runs

Lot #	Concentration 10^{15} Atoms/cc	$\frac{P}{P_o}$	$\frac{I_{sc}}{I_{sco}}$	$\frac{V_{oc}}{V_{oco}}$	Resistivity (Ωcm)
1	200-400	0.87	0.95	0.96	3.5-4.0 Poly-crystalline
23	<20-140	0.96	0.98	0.97	4.6-3.6

NOTES: Small degradation for the single crystal lot; additional degradation in lot #1 probably due to polycrystalline effects.

TABLE 15

Summary of Iron Impurity Runs

Lot #	Concentration 10^{15} Atoms/cc	$\frac{P}{P_o}$	$\frac{I_{sc}}{I_{sco}}$	$\frac{V_{oc}}{V_{oco}}$	Resistivity (Ωcm)
24	0.8	0.86	0.88	1.03	0.16-0.15
30	1.0	S 0.91 C 0.87 T 0.74	0.95 0.90 0.77	1.00 0.99 0.96	5.8-5.0 Gross lineage

NOTES: No apparent difference in degradation between low and high resistivity ingot; noted a sharp degradation in characteristics towards the tang end of ingot for lot #30.

TABLE 16

2.3.7 Summary of Manganese Impurity Runs

Lot #	Concentration 10^{15} Atoms/cc	$\frac{P}{P_o}$	$\frac{I_{sc}}{I_{sco}}$	$\frac{V_{oc}}{V_{oco}}$	Resistivity (Ωcm)
Mn					
5	0.63	0.83	0.89	0.94	4.2-4.9
6	1.0	0.77	0.87	0.92	2.8-4.2
7	0.66	0.83	0.88	0.94	4.9-5.3
10	0.7	0.87	0.90	1.02	0.21-0.2
11	0.63	0.86	0.92	0.95	4.6 Slow growth
Cr-Mn-Ti					
19	0.4/0.5/0.0033	0.73	0.82	0.91	5.5-5.2
Cr-Mn-Ni Ti-V					
26	0.08/0.08/0.5 0.00033/0.0006	0.84	0.89	0.94	4.4
27	0.4/0.4/2.0 0.0024/0.004	0.67	0.76	0.88	5.0-3.8

NOTES: The variations in performance from lot to lot is small, indicating that the processing is consistent. The lower resistivity lot shows less degradation than several other high resistivity lots containing less Mn. Lots #19 and #27 are most severely degraded, probably because of the presence of Ti.

3.0 CONCLUSIONS AND RECOMMENDATIONS

The initial verification lots used control silicon of 1 to 3 Ωcm, typical of terrestrial solar cell production. It was not until after finishing the first five test lots that we learned that all of the test lots were from the Westinghouse/Dow-Corning Program and, therefore, were clustered either in the 0.2 to 0.25 Ωcm or the 3 to 5 Ωcm ranges. Data on control cells of these resistivities would be extremely valuable in performing statistical analysis of the effects of impurities on the various cell parameters. It is only with this type of analysis that the actual mechanisms for performance degradation can be determined unambiguously. Without these runs, it cannot be completely clear as to how much of the performance difference in the test runs was due to bulk silicon resistivity. There is ample evidence that the performance degradation was principally due to impurity contamination and, indeed, a consistent picture emerges for some impurities of a definite dependence on impurity concentration. In several instances, addition of a second impurity to an otherwise innocuous impurity is the cause for definite additional degradation. It can be concluded that certain impurities such as titanium, tantalum and vanadium are particularly bad in this regard even for small concentrations. Cell performance appears relatively tolerable to impurities such as copper, carbon, calcium, chromium, iron and nickel in

the concentration levels which were supplied to us.

We feel that this program has been valuable in verifying the Westinghouse-Dow-Corning work and in evaluating the performance of impurity incorporated samples using a higher baseline efficiency process.

REFERENCES

1. R. H. Hopkins, et al, "Silicon Materials Task of the Low Cost Solar Array Project (Part 2), 9th Quarterly Reports. ERDA/JPL-954331-78/1, 1978.

2. H. W. Gutsche and D. E. Hill, "Determination of a Definition of Solar Grade Silicon", Final Report, No. ERDA/JPL-954338-76.

3. F. A. Lindholm, J. G. Fossum and E. L. Bugess,"Applications of the Super Position Principle to Solar-Cell Analysis" IEEE Trans. Electron Devices, Vol. ED-26, No. 3, March 1979.

4. F. A. Lindholm, A. Neugroschel, C. T. Sah, M. P. Godlewski and H. W. Brandhorst, Jr. "A Methodology for Experimentally Based Determination of Gap Shrinkage and Effective Lifetimes in the Emitter and Base of p-n Junction Solar Cells and other p-n Junction Devices" IEEE Trans. Electron Devices, Vol. ED-24, No. 4, April 1977.

5. A Neugroschel, F. A. Lindholm, and C. T. Sah, "A Method for Determining the Emitter and Base Lifetimes in p-n Junction Diodes", IEEE Trans. Electron Devices, Vol. ED-24, No. 6, June 1977.

6. G. Storti, S. Johnson, H. Lin and R. Armstrong, "Photovoltaic Mechanisms in Polycrystalline Thin Film Solar Cells", Second Quarterly Report, DOE Contract ET-78-0-01-3413, March 1979.

7. R. H. Hopkins, et al, "Effect of Impurities and Processing on Silicon Solar Cells", Phase II Summary and Eleventh Quarterly Report, DOE/JPL-954331-78/3, 1978.

Appendix

Included in this appendix are test wafer data of Lots E-20 through E-31 and also baseline Lot E-39. Test wafer data for earlier lots were included in the three quarterly reports.

Lot No.: E-20 Test

Cell #	I_{sc}(mA)	V_{oc}(mV)	P_m(mW)	I_{mp}(mA)	V_{mp}(mV)	I_{sc} blue(mA)	I_{sc} red(mA
1s	127	542	36	91	395	37	66
2s	130	544	56	121	460	38	64
3s	130	540	53	116	450	39	64
4s	134	546	54	122	445	37	67
5c	130	540	56	122	455	39	63
6c	128	538	52	117	450	39	62
7c	127	539	54	118	455	39	61
8c	128	540	54	119	455	39	61
9c	129	540	55	119	460	38	63
10t	127	538	54	118	460	38	61
11t	125	537	52	115	450	38	60
12t	128	539	51	116	440	39	62
13t	124	538	53	116	455	39	59
X	128.3	539.9	53.7	118.3	452.9	38.5	62.3
S	2.6	2.6	1.6	2.4	6.2	0.67	2.1
V	0.020	0.0048	0.029	0.020	0.014	0.018	0.034
FF =	77.5%						
12 cells							

Lot No.: E-21 Test

Cell #	I_{sc}(mA)	V_{oc}(mV)	P_m(mW)	I_{mp}(mA)	V_{mp}(mV)	I_{sc} blue mA)	I_{sc} red (mA)
1s	86	493	32	78	410	35	30
2s	89	496	34	81	415	37	30
3s	-----	-----	-----	-----	-----	-----	-----
4s	-----	-----	-----	-----	-----	-----	-----
5c	87	494	32	80	405	36	30
6c	88	493	33	81	410	37	30
7c	-----	-----	-----	-----	-----	-----	-----
8c	-----	-----	-----	-----	-----	-----	-----
9t	86	491	32	79	410	36	29
10t	85	491	31	76	410	35	29
11t	87	492	32	78	405	35	30
$\bar{X}$	86.9	492.9	32.3	79.0	409.3	35.9	29.7
S	1.3	1.8	1.0	1.8	3.5	0.90	0.49
V	0.016	0.0036	0.030	0.023	0.0084	0.025	0.016
FF =	75.4%						

Lot No.: E-22 Test

Cell #	I_{sc}(mA)	V_{oc}(mV)	P_m(mW)	I_{mp}(mA)	V_{mp}(mV)	I_{sc} blue(mA)	I_{sc} red(mA)
1s	-----	-----	-----	-----	-----	-----	-----
2s	84	547	30	69	445	34	29
3s	86	558	36	76	470	35	31
4s	85	563	34	72	480	36	29
5c	-----	-----	-----	-----	-----	-----	-----
6c	86	567	37	78	475	36	30
7c	87	564	34	72	475	37	29
8c	86	568	37	77	480	36	30
9c	82	566	35	73	480	37	30
10c	84	559	32	71	460	36	29
11t	85	566	36	75	480	37	29
12t	45	565	--	--	---	19	15
$\overline{X}$	85.5	562.3	34.9	74.3	472.0	36.2	29.6
S	2.1	6.3	2.5	3.5	11.4	1.1	0.70
V	0.025	0.011	0.071	0.047	0.024	0.031	0.024
FF =	72.6%						

Lot No.: E-23 Test

Cell #	I_{sc} (mA)	V_{oc} (mV)	P_m (mW)	I_{mp} (mA)	V_{mp} (mV)	I_{sc} blue (mA)	I_{sc} red (mA)
1	------	----------	----------	-Broken--	----------	----------	----------
2	146	574	67	139	480	36	78
3	------	----------	----------	-Broken--	----------	----------	----------
4	149	575	68	140	485	38	79
5	------	----------	----------	-Broken--	----------	----------	----------
6	147	575	67	139	485	37	78
7	147	576	67	139	485	37	78
8	146	578	67	138	485	37	78
9	148	576	68	139	490	38	78
10	147	577	65	137	475	38	78
11	148	578	68	141	485	38	78
12	------	----------	----------	-Broken--	----------	----------	----------
8 cells							
$\overline{X}$	147.2	576.1	67.1	139.0	483.8	37.4	78.1
S	1.0	1.5	1.0	1.2	4.4	0.74	0.35
V	0.0070	0.025	0.015	0.0086	0.0092	0.020	0.0045
FF	79.1%						

Lot No.: E-24 Test

Cell #	I_{sc} (mA)	V_{oc} (mV)	P_m (mW)	I_{mp} (mA)	V_{mp} (mV)	I_{sc} blue (mA)	I_{sc} red (mA)
1s	134	616	64	123	520	39	68
2s	132	611	58	114	505	38	67
3s	133	612	60	115	525	39	67
4c	------	------	------	------	------	------	------
5c	------	------	------	------	------	------	------
6c	131	614	60	117	520	39	66
7c	135	613	63	121	520	40	68
8c	------	------	------	------	------	------	------
9c	130	610	56	110	510	40	64
10c	131	610	59	115	515	40	65
11t	------	------	------	------	------	------	------
12t	128	610	58	114	510	40	63
13t	------	------	------	------	------	------	------
8 cells							
$\bar{X}$	131.8	612.0	59.8	116.1	515.6	39.4	66.0
S	2.3	2.2	2.7	4.2	6.8	0.74	1.9
V	0.017	0.0036	0.044	0.036	0.013	0.019	0.028
FF	74.1%						

Lot No.: E-25 Test

Cell #	I_{sc} (mA)	V_{cc} (mV)	P_m (mW)	I_{mp} (mA)	V_{mp} (mV)	I_{sc} blu (mA)	I_{sc} red (mA)
1s*	90	495	34	83	405	30	37
2s**	95	500	37	88	415	32	39
3s	91	498	36	85	425	31	37
4s	91	498	36	85	425	31	37
5c	91	497	36	85	420	31	37
6c	91	499	35	85	420	31	37
7c	89	497	35	83	420	29	38
8c*	95	494	32	77	415	33	37
9c	93	497	36	86	415	32	37
10t*	92	492	31	75	410	32	37
11t	92	493	33	80	415	32	35
12t**	88	487	28	79	395	31	34
13t	90	493	32	77	415	32	36
*ONE CORNER MISSING							
**TWO CORNERS MISSING							
$\overline{X}$	91.4	495.4	33.9	82.2	415.0	31.3	36.8
S	2.1	3.5	2.6	4.1	8.2	1.0	1.2
V	0.023	0.0072	0.077	0.050	0.020	0.033	0.034
FF	74.9%						

Lot No.: E-26 Test

Cell #	I_{sc}(mA)	V_{oc}(mV)	P_m(mW)	I_{mp}(mA)	V_{mp}(mV)	$I_{sc\ blue}$(mA)	$I_{sc\ red}$(mA)
1s	135	566	60	126	475	35	70
2s	137	565	62	130	475	35	70
3s	134	561	59	125	470	36	68
4c	133	561	59	125	470	35	67
5c	134	557	58	124	470	37	67
6c	135	562	58	125	465	36	69
7c	134	564	60	127	475	34	69
8c	135	562	59	128	490	37	68
9c	139	563	59	128	460	36	71
10c	135	560	57	123	465	36	69
11c	---FRONT REJECT---						
12t	132	550	53	117	455	37	67
13t	132	557	57	122	465	35	67
11 cells							
X	134.6	560.7	58.4	125.0	469.6	35.8	68.5
S	2.0	4.4	2.2	3.4	8.9	1.0	1.4
V	0.015	0.0078	0.038	0.027	0.019	0.027	0.020
FF	77.4%						

Lot No.: E-27 Test

Cell #	I_{sc}(mA)	V_{oc}(mV)	P_m(mW)	I_{mp}(mA)	V_{mp}(mV)	I_{sc} blue (mA)	I_{sc} red (mA)
1s	114	529	48	108	495	38	47
2s	113	526	46	105	490	37	48
3s	114	529	48	107	495	37	48
4s	114	527	47	104	500	38	48
5c	114	528	47	108	490	38	48
6c	116	529	48	109	490	38	49
7c	114	525	47	105	495	37	48
8c	114	527	47	106	495	39	47
9t	114	525	46	106	485	38	48
10t	113	525	46	106	485	37	47
11t	113	524	47	106	490	38	47
12t	114	525	47	108	485	37	48
$\overline{X}$	113.9	526.6	47.0	106.5	491.3	37.7	47.8
S	0.79	1.8	0.74	1.5	4.8	0.65	0.62
V	0.0070	0.0035	0.016	0.014	0.0098	0.017	0.013
FF	78.4%						

Lot No.: E-28 Test

Cell #	I_{sc}(mA)	V_{oc}(mV)	P_m(mW)	I_{mp}(mA)	V_{mp}(mV)	I_{sc} blue(mA)	I_{sc} red(mA
1s	145	569	64	136	465	39	76
2s	142	567	62	130	475	38	75
3s	146	561	64	136	470	39	75
4s	144	569	60	134	450	40	75
5c	141	564	60	130	465	40	82
6c	142	570	64	132	480	39	73
7c	138	566	61	128	475	35	72
8c	141	569	63	132	480	37	76
9c	140	569	62	130	480	35	75
10t	141	568	62	130	480	36	76
11t	139	568	62	130	475	35	75
12t	139	564	62	130	475	36	73
13t	141	567	63	131	480	38	75
13 cells							
$\bar{X}$	141.5	567.0	62.2	131.5	473.1	37.5	75.2
S	2.4	2.6	1.4	2.5	8.8	1.9	2.4
V	0.017	0.0046	0.022	0.019	0.019	0.051	0.032
FF	77.5%						

Lot No.: E-29 Test

Cell #	I_{sc}(mA)	V_{oc}(mV)	P_m(mW)	I_{mp}(mA)	V_{mp}(mV)	I_{sc} blue(mA)	I_{sc} red(mA)
1s	113	558	50	107	465	34	55
2s	-----	----------	----------	-BROKEN IN ETCH---		----------	------
3s	115	556	51	107	475	35	56
4c	116	558	51	108	470	35	56
5c	109	556	48	101	475	33	53
6c	110	556	48	101	475	34	53
7c	111	558	47	101	465	34	54
8c	114	554	47	101	460	36	52
9c	118	559	52	110	470	37	56
10c	114	557	50	101	470	35	54
11t	111	556	46	99	465	36	52
12t	111	555	46	97	470	35	52
13t	110	555	47	102	465	35	52
12 cells							
$\bar{X}$	112.7	556.5	48.7	102.9	468.8	34.9	53.8
S	2.8	1.5	2.3	4.0	4.8	1.1	1.7
V	0.025	0.0027	0.047	0.039	0.010	0.031	0.031
FF	77.6%						

Lot No.: E-30 Test

Cell #	I_{sc} (mA)	V_{oc} (mV)	P_m (mW)	I_{mp} (mA)	V_{mp} (mV)	$I_{sc\ blue}$ (mA)	$I_{sc\ red}$ (mA)
1s	142	599	63	126	500	42	68
2s	145	595	64	129	495	42	70
3s	140	596	64	127	500	41	66
$\bar{X}$	142.3	596.7	63.7	127.3	498.3	41.7	68.0
S	2.5	2.1	0.58	1.5	2.9	0.58	2.0
V	0.018	0.0035	0.0091	0.012	0.0058	0.014	0.029
FF	75.0%						
4c	144	597	62	125	500	42	68
5c	146	595	65	132	495	42	71
6c	145	599	65	130	500	41	71
9c	147	597	66	134	495	42	72
7c	128	584	59	119	495	42	58
8c	120	575	55	113	485	42	51
10c	118	573	53	111	480	41	49
$\bar{X}$	135.4	588.6	60.7	123.4	492.9	41.7	62.9
S	13.0	11.1	5.2	9.3	7.6	0.49	10.0
V	0.095	0.019	0.085	0.075	0.015	0.012	0.16
FF	76.2%						
11t	114	570	51	106	480	41	48
12t	117	570	52	109	480	43	48
13t	118	570	53	110	480	41	50
$\bar{X}$	116.3	570.0	52.0	108.3	480.0	41.7	48.7
S	2.1	0.0	1.0	2.1	0.0	1.2	1.2
V	0.018	0.0	0.019	0.019	0.0	0.028	0.024
FF	78.4%						

Lot No.: E-31 Test

Cell #	I_{sc} (mA)	V_{oc} (mV)	P_m (mW)	I_{mp} (mA)	V_{mp} (mV)	I_{sc} blue (mA)	I_{sc} red (mA)
1s	127	557	54	118	455	39	60
2s	130	561	54	120	450	40	61
3s	133	556	54	120	450	42	62
4s	131	563	57	122	470	39	64
5c	129	557	54	117	460	40	61
6c	129	557	54	117	460	40	61
7c	122	554	53	114	465	33	62
8c	124	555	54	115	465	34	62
9c	127	558	55	118	465	35	64
10t	125	555	48	109	435	36	62
11t	124	553	54	114	470	36	62
12t	124	555	53	115	460	34	63
13t	129	559	54	117	460	37	64
X	127.2	556.9	53.7	116.6	458.8	37.3	62.2
S	3.3	2.8	2.0	3.3	9.6	2.9	1.3
V	0.26	0.0051	0.037	0.029	0.021	0.077	0.021
FF	75.8%						

Lot No.: E-39 Test

Cell #	I_{sc} (mA)	V_{oc} (mV)	P_m (mW)	I_{mp} (mA)	V_{mp} (mV)	$I_{sc\ blue}$ (mA)	$I_{sc\ red}$ (mA)
1	150	576	68	143	475	41	79
2	148	575	68	137	490	40	78
3	148	574	67	140	475	40	78
4	---------------------------BROKEN IN SAW---------------------------						
5	147	573	65	135	480	40	79
6	149	573	68	142	475	43	78
7	150	576	69	144	475	41	79
8	150	577	68	140	485	43	78
9	148	574	68	142	480	41	78
10	150	575	70	145	475	43	78
11	151	577	68	143	480	42	78
12	148	573	67	137	490	41	78
13	149	576	68	140	485	41	77
X	149.0	574.9	67.8	140.7	480.4	41.3	78.2
S	1.2	1.5	1.2	3.1	5.8	1.2	0.58
V	0.0081	0.0026	0.018	0.022	0.012	0.028	0.0074
FF	79.2%						